

# Conformation of (*S*-Glutathionato)(2,2':6',2''-terpyridine)platinum(II) Ion, [Pt(trpy)GS]<sup>+</sup>, Determined from Cross-Relaxation Effects in Two-Dimensional <sup>1</sup>H NMR Spectra. Importance of Ligand–Ligand Hydrophobic Interactions in Metal–Peptide Complexes

Nenad Juranić,\*† Vladimir Likić,† Nenad M. Kostić,‡ and Slobodan Macura†

Department of Biochemistry and Molecular Biology, Mayo Graduate School, Mayo Clinic and Foundation, Rochester, Minnesota 55905, and Department of Chemistry, Iowa State University, Ames, Iowa 50011

Received July 12, 1994<sup>⊗</sup>

The tripeptide glutathione binds to the platinum(II) atom via the thiolato anion in the cysteine side chain. Conformation of the complex [Pt(trpy)GS]<sup>+</sup> dissolved in a mixture of dimethylformamide-*d*<sub>7</sub> and water at –15 °C is determined by a combination of molecular-mechanics calculations, molecular-dynamics calculations, and two-dimensional cross-relaxation <sup>1</sup>H NMR spectroscopy. The viscous solvent and low temperature bring the complex into the spin-diffusion regime, so that cross-relaxation rates can accurately be determined. Interproton distances obtained from these rates serve as constraints in the minimization of molecular potential energy by standard methods. There are hydrophobic interactions between the glutamyl methylene groups in the glutathionato ligand and a terminal pyridine ring in the terpyridine ligand. This interaction excludes the most hydrophobic part of the glutathionato ligand from the polar solvent. Similar interactions may be responsible for the useful dependence of the UV–visible spectroscopic features of the [Pt(trpy)L]<sup>2+/+</sup> chromophore, attached to the side chain L in proteins, on the environment of this side chain. Conformation of the glutathionato ligand in [Pt(trpy)GS]<sup>+</sup> differs from the conformation of free glutathione in solution. This finding may be relevant to binding of glutathione to many enzymes that depend on it. This is an early, and promising, application of two-dimensional cross-relaxation NMR spectroscopy to stereochemistry of metal complexes.

## Introduction

Many important chemical and biological phenomena are governed by hydrophobic interactions. A few are enzyme-substrate association, assembly of lipids into membranes, surfactant aggregation, and kinetic solvent effects.<sup>1</sup> Recent studies showed the importance of hydrophobic interaction for the conformations of short linear peptides in solution<sup>2</sup> and for the structures of transition-metal complexes.<sup>3</sup> Very recent studies implicated hydrophobic forces in stabilizing transient structures in the initial steps of protein folding.<sup>4</sup> Because many proteins contain metal ions, conformations of metal–peptide complexes are important and worthy of systematic study. In this report we examine interactions between a peptide and other ligands in the coordination sphere of a metal ion.

Established methods for the study of ligand–ligand interactions in dissolved metal complexes are based on the changes in stability of complexes, changes in the electronic absorption spectra, and shifts of NMR resonances. Useful as these methods are, they reveal only indirectly the stereochemical aspects of ligand–ligand interactions. These standard methods do not show the most interesting feature of coordinated peptides—their conformation. A more direct method would involve determination of interproton distances on the basis of nuclear Overhauser effects (NOE) in two-dimensional NMR experiments. This

cross-relaxation NMR spectroscopy has proven its great value in structural studies of macromolecules, but its application to relatively small molecules is severely limited by two general factors. First, macromolecules have long correlation times and fast cross-relaxation, whereas small molecules have short correlation times and very slow cross-relaxation. Measurement of these low cross-relaxation rates is especially difficult because cross-relaxation is accompanied by overall relaxation. Second, the number of observable interproton “contacts” is much greater in macromolecules than in small molecules. Structure of a macromolecule can be precisely determined on the basis of many contacts even if the corresponding distances are only approximate. The structure of a small molecule, however, can be determined only if the interproton distances, which are relatively few, are known exactly. Estimates of cross-relaxation rates are sufficient in the study of macromolecules, but accurate measurements are required in the study of small molecules.

Cross-relaxation rate constants are best determined when the system exists in the spin-diffusion regime. Macromolecules, by virtue of their large mass, satisfy this requirement already at room temperature. Small molecules, however, need to be brought into the spin-diffusion regime by a combination of a viscous solvent and cooling, so that the correlation time for molecular tumbling lengthens to nanoseconds. Since many common liquids freeze at relatively high temperatures, various solvent mixtures must be used to bring dissolved small molecules into the spin-diffusion regime. For these reasons, structural study of small molecules on the basis of cross-relaxation rates is possible only in solvent mixtures and at low temperatures. We know of only three previous studies in which nuclear Overhauser effects in transition-metal complexes were amplified by use of viscous solvents.<sup>5–7</sup> Cross-relaxation

\* Author to whom correspondence should be addressed.

† Mayo Clinic and Foundation.

‡ Iowa State University.

<sup>⊗</sup> Abstract published in *Advance ACS Abstracts*, February 1, 1995.

- (1) Blokzijl, W.; Engberts, J. *Angew. Chem., Int. Ed. Engl.* **1993**, *32*, 1545–1579.
- (2) Dyson, J.; Wright, P. *Annu. Rev. Biophys. Biophys. Chem.* **1991**, *20*, 519–538.
- (3) Sigel, H. *Pure Appl. Chem.* **1989**, *61*, 923–932.
- (4) Dyson, J.; Wright, P. *Curr. Opin. Struct. Biol.* **1993**, *3*, 60–65.

(5) Luck, L. A.; Landis, R. *Organometallics* **1992**, *11*, 1003–1005.

spectroscopy is only beginning to show its promise in stereochemical investigations of metal-peptide complexes, and our study is an early undertaking in this new area.

The complex (*S*-glutathionato)(2,2':6',2''-terpyridine)platinum(II), [Pt(trpy)GS]<sup>+</sup>, is well suited for stereochemical study by NMR spectroscopy. One ligand in it is aliphatic, and the other is aromatic. Hydrophobic interactions between such molecules (in this case they are ligands in the same complex) are enhanced by addition of organic solvents to an aqueous solution.<sup>3</sup> With the suitable organic solvent, this addition at the same time yields a viscous cryoprotective solvent required for restricting molecular motions. Platinum(II) complexes are well-known for their thermodynamic stability and inertness to ligand substitution. These desirable properties are enhanced because terpyridine is a tridentate ligand and because the thiolate side chain in the peptide has a high affinity for the soft platinum(II) atom.

Study of [Pt(trpy)GS]<sup>+</sup> is of interest to bioinorganic chemists. Reactions of [Pt(trpy)Cl]<sup>+</sup> with proteins result in displacement of the chloride ion and selective attachment of the Pt(trpy)<sup>2+</sup> group to exposed histidine, cysteine, and certain arginine side chains.<sup>8–15</sup> Selectivity of this binding and spectroscopic properties of the Pt(trpy)<sup>2+</sup> chromophore depend on its noncovalent as well as covalent interactions with the proteins. When [Pt(trpy)Cl]<sup>+</sup> acts as a reversible inhibitor for enzymes, the chromophore interacts with the active site and can be used as a probe of this site.<sup>16</sup>

Conformation of glutathione in solution has long interested theorists and experimentalists.<sup>17</sup> Changes of this conformation upon binding of glutathione to other molecules is especially interesting because it has been suggested that the structure of the active site of glyoxalase I may be adapted to fit the most stable structure of free glutathione in solution.<sup>18</sup> Our study pertains also to this question.

## Structure Determination

**Theoretical Basis of the Method.** Cross-relaxation is a process of magnetization transfer among nuclear spins, induced by nuclear magnetic dipole–dipole interaction. Cross-relaxation can be observed in both the laboratory frame and the rotating frame of reference. The basic theoretical description of cross-relaxation in both frames is well-known.<sup>19</sup> The most important experimental manifestation of cross-relaxation is the nuclear Overhauser effect (NOE).<sup>20,21</sup> It is the change in the intensity of one spectral line when another line is perturbed by a

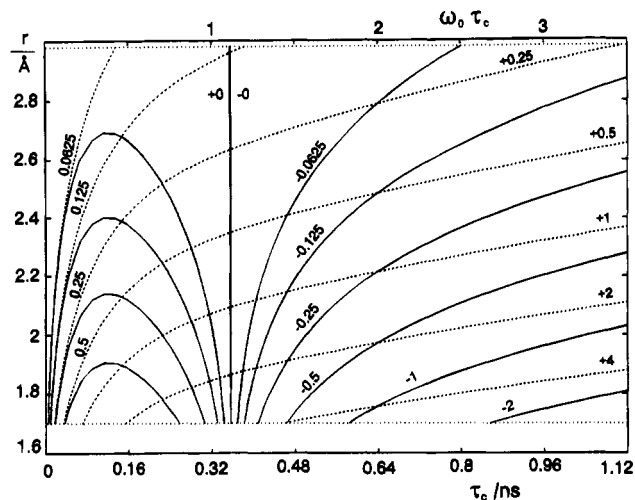


**Figure 1.** Dependence of cross-relaxation rates on correlation time,  $\tau_c$ , and interproton distances,  $r$ , at  $\omega_0/2\pi = 500$  MHz in the laboratory frame (NOESY, —) and in the rotating frame (ROESY, - -). Numbers along the contours are the corresponding cross-relaxation rate constants, in  $s^{-1}$ .

radiofrequency field. The nuclear Overhauser effect, too, can be observed in both the laboratory frame and the rotating frame of reference. Nuclear Overhauser effects (or cross-relaxation rates) are most suitably measured by two-dimensional (2D) spectroscopy<sup>22</sup> because this technique allows simultaneous monitoring of interactions among all nuclear spins. The experiment in the laboratory frame<sup>23</sup> is known as 2D NOE or NOESY (nuclear Overhauser effect spectroscopy), and the experiment in the rotating frame,<sup>24</sup> as 2D ROE or ROESY (rotating frame Overhauser effect spectroscopy). Cross-relaxation is a first-order process, characterized by the rate constant  $\sigma$ . Because NOE can be positive or negative, i.e., because the line intensity can either increase or decrease upon perturbation of another line, cross-relaxation rate constants can be considered as positive or negative. Cross-relaxation rates between spins  $k$  and  $l$ , experimentally measured in the laboratory frame  $\sigma_{kl}^n$ , or in the rotating frame  $\sigma_{kl}^r$ , depend on the interspin distance,  $r_{kl}$ , and on the correlation time,  $\tau_c$ , that modulates dipole-dipole interaction according to eqs 1 and 2.<sup>19</sup> The

$$\sigma_{kl}^n = f^n(\tau_c)r_{kl}^{-6} \quad (1)$$

$$\sigma_{kl}^r = f^r(\tau_c)r_{kl}^{-6} \quad (2)$$

functions  $f^n(\tau_c)$  and  $f^r(\tau_c)$  depend on the type of molecular motion, and they are well defined for a rigid body with isotropic motion.<sup>19</sup> Figure 1 shows cross-relaxation rates in the laboratory frame as a contour plots of correlation time and interproton distances, according to eqs 1 and 2, for a spin pair in a rigid, isotropically moving body. The time scale is linear and spans the range expected for the correlation times of coordination compounds, 0.01–1.4 ns. For  $\omega_0\tau_c > 1.12$  ( $\omega_0$  is NMR resonance frequency in rad/s),  $\sigma^n$  is negative, proportional to the correlation time, and inversely proportional to the sixth

(6) Giovannetti, J. S.; Kelly, C.; Landis, C. *J. Am. Chem. Soc.* **1993**, *115*, 4040–4057.

(7) Juranić, N.; Likić, V.; Parac, T.; Macura, S. *J. Chem. Soc., Perkin Trans. 2* **1993**, 1805–1810.

(8) Ratilla, E. M. A.; Brothers, H. M. I.; Kostić, N. M. *J. Am. Chem. Soc.* **1987**, *109*, 4592–4599.

(9) Brothers, H. M. I.; Kostić, N. M. *Inorg. Chem.* **1988**, *27*, 1761–1767.

(10) Ratilla, E. M. A.; Kostić, N. M. *J. Am. Chem. Soc.* **1988**, *110*, 4427–4428.

(11) Kostić, N. M. *Comments Inorg. Chem.* **1988**, *8*, 137–162.

(12) Zhou, X. Y.; Kostić, N. M. *Polyhedron* **1990**, *9*, 1975–1983.

(13) Ratilla, E. M. A.; Kostić, N. M. *J. Serb. Chem. Soc.* **1992**, *57*, 205–215.

(14) Pinnow, S. L.; Brothers, H. M. I.; Kostić, N. M. *Croat. Chem. Acta* **1991**, *64*, 519–528.

(15) Peerey, L. M.; Kostić, N. M. *Inorg. Chem.* **1987**, *26*, 2079–2083.

(16) Kostić, N. M.; Brothers, H. M., II *Biochemistry* **1990**, *29*, 7468–7474.

(17) Podanyi, B.; Reid, S. *J. Am. Chem. Soc.* **1988**, *110*, 3805–3810.

(18) Rosevear, P.; Sellin, S.; Mannervik, B.; Kuntz, I.; Mildvan, A. *J. Biol. Chem.* **1984**, *259*, 11436–11447.

(19) Solomon, I. *Phys. Rev.* **1955**, *99*, 559–565.

(20) Noggle, J. H.; Schirmer, R. E. *The Nuclear Overhauser Effect in Chemical Applications*, Academic Press: New York, 1971.

(21) Neuhaus, D.; Williamson, M. *The Nuclear Overhauser Effect in Structural and Conformational Analysis*; VCH Publishers: New York, 1989.

(22) Ernst, R. R.; Bodenhausen, G.; Wokaun, A. *Principles of Nuclear Magnetic Resonance in One and Two Dimensions*; Oxford University Press: New York, 1987.

(23) Macura, S.; Ernst, R. R. *Mol. Phys.* **1980**, *41*, 95–117.

(24) Bothner-By, A. A.; Stephens, R. L.; Lee, J.; Warren, C. D.; Jeanloz, R. W. *J. Am. Chem. Soc.* **1984**, *106*, 811–813.

power of the interspin distance. At  $\omega_0\tau_c \approx 1.12$ , the cross-relaxation vanishes; i.e.,  $\sigma^n$  is zero. For  $\omega_0\tau_c < 1.12$ ,  $\sigma^n$  is positive and shows a distinct maximum at  $\omega_0\tau_c \approx 0.382$ .

Cross-relaxation rate in the rotating frame (dashed lines in Figure 1) monotonically increases with correlation times. For  $\omega_0\tau_c < 0.382$ , both cross-relaxation rates,  $\sigma^n$  and  $\sigma^r$ , similarly depend on correlation time. When  $\omega_0\tau_c$  approaches zero, the quotient  $\sigma^n/\sigma^r$  approaches unity. When  $\omega_0\tau_c \gg 1$ , both cross-relaxation rates increase monotonically and are proportional to correlation time. In this regime, known as spin-diffusion limit,  $\sigma^n$  is negative and  $\sigma^r$  is positive, with a constant limiting quotient  $\sigma^n/\sigma^r = -1/2$ .<sup>25</sup>

**Measurement of Cross-Relaxation Rate Constants.** Two-dimensional cross-relaxation spectrum recorded at the mixing time  $\tau_m$  can be represented as a matrix  $\mathbf{a}(\tau_m)$ , the elements of which are cross-peak volumes,  $a_{kl}(\tau_m)$ . The matrix  $\mathbf{a}(\tau_m)$  depends in an exponential way on the relaxation matrix,  $\mathbf{R}$ , the elements of which are cross-relaxation rates,  $\sigma_{kl}$ .<sup>23</sup> This dependence is shown in eq 3. A diagonal matrix  $\mathbf{a}(0)$  represents

$$\mathbf{a}(\tau_m) = e^{-\mathbf{R}\tau_m} \mathbf{a}(0) \quad (3)$$

the spectrum at  $\tau_m = 0$ . Individual cross-relaxation rates,  $\sigma_{kl}$ , can be obtained directly from eq 3 by a full matrix analysis.<sup>26–28</sup> Alternatively, cross-relaxation rates can be obtained by polynomial expansion of eq 4<sup>23</sup> and by normalization of cross-peak

$$\frac{a_{kl}(\tau_m)}{0.5[a_{kk}(\tau_m) + a_{ll}(\tau_m)]} \approx -\sigma_{kl}\tau_m + \frac{1}{2} \sum_{j \neq k,j} \sigma_{kj}\sigma_{jl}\tau_m^2 \quad (4)$$

volumes,  $a_{kl}(\tau_m)$ , by respective diagonal-peak volumes  $a_{kk}(\tau_m)$  and  $a_{ll}(\tau_m)$ .<sup>29,30</sup> The cross-relaxation rate,  $\sigma_{kl}$ , is extracted from the buildup curve, eq 4, by polynomial (quadratic or cubic) least-squares fit. The main advantage of eq 4 is that it recovers cross-relaxation rates from partially resolved spectra. A disadvantage is that it requires several experiments, with different mixing times.

**Determination of Interproton Distances.** Interproton distances can be calculated directly from eq 1, according to eq 5. This last equation is of limited value because an estimate of

$$r_{kl} = \left( \frac{f(\tau_c)}{\sigma_{kl}} \right)^{1/6} \quad (5)$$

$f(\tau_c)$  usually is unavailable. For determination of an interproton distance, dependence on correlation time must be eliminated. Most commonly, this is done by comparing the cross-relaxation rate  $\sigma_{std}$  of a spin pair at a known distance  $r_{std}$  with the cross-relaxation rate  $\sigma_{kl}$  between spins separated by measured interspin distances,  $r_{kl}$ ; see eq 6. If the correlation-time function,  $f(\tau_c)$ ,

$$r_{kl} = r_{std} \left( \frac{\sigma_{std}}{\sigma_{kl}} \right)^{1/6} \quad (6)$$

is the same for all spin pairs, it is sufficient to measure the

cross-relaxation rate in either the laboratory frame or the rotating frame. At the spin-diffusion limit,  $f(\tau_c)$  has the largest value, and consequently cross-relaxation in both frames is fastest then. Even more important, at the spin-diffusion limit in the laboratory frame cross-relaxation is much faster than the overall relaxation, and thus cross-relaxation can be measured with the highest accuracy. To bring a system into the spin-diffusion regime it is necessary to increase correlation time for molecular reorientation. This can be achieved by cooling and by use of viscous solvents. The two effects are usually combined when a liquid or a mixture of liquids with a low freezing point (cryoprotective solvent) also has a high viscosity. For coordination compounds in cryoprotective solvents of high viscosity, cooling to below 0 °C yields  $\tau_c$  of 1–5 ns. In a magnetic field of 11 T, for which  $\omega_0/2\pi = 500$  MHz, the system reaches the spin-diffusion limit with  $\omega_0\tau_c = 3–15$ .

**Structure Building from Distance Constraints.** Geometry of an object, up to the mirror symmetry, can in principle be reconstructed from the distances among its elements. Because of the  $r^{-6}$  dependence, cross-relaxation measurements provide only distances shorter than 5 Å. These distances are only a small fraction of all the distances in a typical molecule. Although interproton distances derived from NMR experiments are not sufficient for reconstruction of a molecule, they can be used to select among possible conformations of this molecule of known chemical composition. The standard procedure for conformational analysis involves restrained minimization of molecular energy (MM) and restrained molecular dynamics (rMD).<sup>31</sup>

## Experimental Procedures

**Preparation of [Pt(trpy)GS]Cl.** The compound [Pt(trpy)Cl]Cl·2H<sub>2</sub>O was obtained from Aldrich Chemical Co.; it can also be prepared by a published procedure.<sup>32</sup> Glutathione in the reduced form,  $\gamma$ -Glu-Cys-Gly, was obtained from Sigma Chemical Co. To a stirred solution of 532 mg (1.0 mmol) of [Pt(trpy)Cl]Cl·2H<sub>2</sub>O in the minimal volume of water was dropwise added a concentrated aqueous solution of 307 mg (1.0 mmol) of reduced glutathione. The color changed already during the mixing. The reaction mixture was stirred overnight, at room temperature. The complex salt [Pt(trpy)GS]Cl was precipitated with ethanol, removed by filtration, washed by ethanol, and dried in air. Thin-layer chromatography with 0.10 M HCl as an eluent showed a single spot—an indication of purity. This procedure is essentially identical to a published one.<sup>9</sup> For NMR measurements, a 10 mM solution of the complex salt was made in a 1:1 mixture by volume of H<sub>2</sub>O adjusted to pH 3.0 by HCl and dimethylformamide-*d*<sub>7</sub>.

**NMR Spectroscopy.** Spectra were recorded at 500 MHz on a Bruker AMX-500 instrument. Pure absorption NOESY and ROESY ( $B_1 = 3$  kHz) spectra were obtained by time-proportional phase incrementation.<sup>33</sup> There were 512 free-induction decays (FID) of 2048 data points, with 32 scans for each point. The repetition time was 3 s, and spectral width was 4500 Hz in both dimensions. The spectra were processed with FELIX 2.0 (Hare Research, Inc., 1991) on a Silicon Graphics workstation. Gaussian filters were used in both dimensions (GB1 = 0.2, LB1 = -2, GB2 = 0.02, and LB2 = -2). After zero-filling, the spectral matrices consisted of 2048 × 2048 real points. Before volume integration, the baseplane was corrected by a linear prediction of the first point in the FID. Peak volumes were exported to MATLAB (The Math Works, Inc., 1992) and fitted by quadratic function according to eq 4.<sup>34</sup>

The proton spectrum is assigned from two-dimensional double-

(25) Farmer, B. T., II; Macura, S.; Brown, L. R. *J. Magn. Reson.* **1988**, *80*, 1–22.

(26) Bremer, J.; Mendz, G. L.; Moore, W. J. *J. Am. Chem. Soc.* **1984**, *106*, 4691–4696.

(27) Boelens, R.; Koning, T. M. G.; Van der Marel, G. A.; Van Boom, J. H.; Kaptein, R. *J. Magn. Reson.* **1989**, *82*, 290–308.

(28) Borgias, B. A.; James, T. L. *Methods Enzymol.* **1989**, *176*, 169–183.

(29) Macura, S.; Farmer, B. T., II; Brown, L. R. *J. Magn. Reson.* **1986**, *70*, 493–499.

(30) Fejzo, J.; Zolnai, Z.; Macura, S.; Markley, J. L. *J. Magn. Reson.* **1990**, *88*, 93–110.

(31) Scheek, R. M.; van Gunsteren, W. F.; Kaptein, R. *Methods Enzymol.* **1989**, *177*, 204–218.

(32) Howe-Grant, M.; Lippard, S. *Inorg. Synth.* **1980**, *20*, 101–106.

(33) Marion, D.; Wüthrich, K. *Biochem. Biophys. Res. Commun.* **1983**, *113*, 967–974.

(34) Fejzo, J.; Zolnai, Z.; Macura, S.; Markley, J. L. *J. Magn. Reson.* **1989**, *82*, 518–528.

quatum filtered correlated spectrum (DQ-COSY),<sup>35</sup> (not shown), in combination with NOE data. Chemically equivalent protons of the terpyridyl ligand where not resolved in the spectrum.

**Structure Determination.** The complex [Pt(trpy)GS]<sup>+</sup> was built in the program CHARMM<sup>36</sup> by applying PATCH between platinum(II), terpyridyl, and the glutathione residue. Distances and angles involving platinum(II) atom were taken from the crystal structure of a closely related (thiolato)(terpyridine)platinum(II) complex.<sup>37</sup> The Pt–N and Pt–S equilibrium distances were set at 2.00 and 2.30 Å, respectively, and the Pt–S–C angle was set at a tetrahedral value. The following force constants were chosen:<sup>38</sup> 300 kcal·mol<sup>-1</sup>·Å<sup>-2</sup> for the Pt–N and Pt–S bonds and 60 kcal·mol<sup>-1</sup>·rad<sup>-2</sup> for the Pt–N–C and Pt–S–C angles, while the angle N–Pt–N energy terms were excluded because some of them approach 180°. Additional energy terms (40 kcal·mol<sup>-1</sup>·rad<sup>-2</sup>) were included to maintain planarity about the platinum(II) atom. The application of the program CHARMM in the subsequent structure determination was limited to the building of initial structure and final energy minimization.

The protein structure file<sup>36</sup> of the complex [Pt(trpy)GS]<sup>+</sup> was exported to the program XPLOR<sup>39</sup> where the annealing procedure with NOE distance restraints was set up. For the purpose of annealing, all masses were set to 100 amu, and all bond and angle force constants were set to 1000 kcal·mol<sup>-1</sup>·Å<sup>-2</sup> and 500 kcal·mol<sup>-1</sup>·rad<sup>-2</sup>, respectively. Improper dihedral force constants were set to 500 kcal·mol<sup>-1</sup>·rad<sup>-2</sup> while dihedral energy terms were excluded. Total energy comprised bond, angle, improper, and Van der Waals energy terms and NOE restraints energy terms in some phases (see below).

A total of 34 NOE distance restraints were used; 31 close contacts and 3 that required the final distance to be >5 Å. The biharmonic potential function was used for close contacts while the square-well function was used for the absent contacts.<sup>39</sup>

The annealing schedule included three phases (20 ps each) of a restrained molecular dynamics (with 0.002 ps time step). In the first phase, the temperature was set to 1000 K and all energy terms that do not include geminal protons were scaled to 5% of their original values. The energy terms involving geminal protons were scaled to 0.1% of their original values. Scaling factors were determined empirically with the purpose to “melt” the structure for the thorough examination of the conformational space. Scaling to 5% of the original energy term values did not allow inversion of chirality at the chiral C atom, while scaling to 0.1% for geminal protons allowed inversion of their prochirality during the annealing. In the first 20 ps of annealing no NOE restraints were imposed. In the next 20 ps of dynamics, temperature and the energy terms were maintained while the NOE restraints were introduced with a low weight. The conformational space was moderately biased in favor of the structures that satisfy NOE restraints. In the third, final phase of restrained molecular dynamics (20 ps), the system was gradually cooled to 300 K while all energy terms were linearly scaled to the 20% of their initial values and NOE restraints were linearly scaled by a factor 20. Finally, the NOE restraints were removed and 1000 steps of the conjugate gradient minimization was performed and the structure was saved. The procedure was looped, so the final structure of one cycle is the initial structure for the another.

Calculations were carried out on Silicon Graphics Indigo<sup>2</sup> workstations.

## Results and Discussion

**Determination of the [Pt(trpy)GS]<sup>+</sup> Structure.** The water–dimethylformamide mixture reaches maximum viscosity, 2.5 times higher than that of water, at 63% by volume of dimethylformamide.<sup>40</sup> Since [Pt(trpy)GS]Cl is sparingly soluble

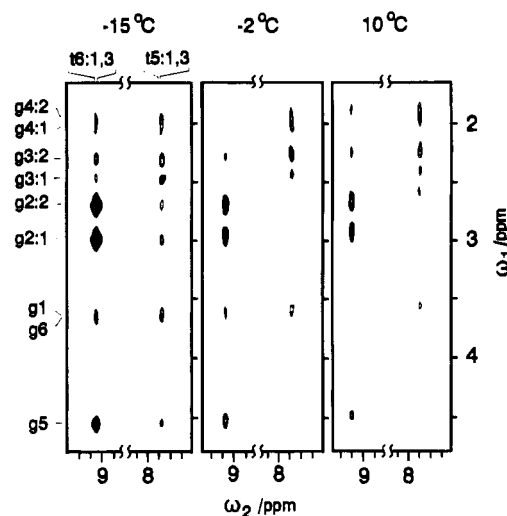


**Figure 2.** Interligand cross-peaks between the terpyridine and glutathione protons in the ROESY spectra of [Pt(trpy)GS]<sup>+</sup> (dissolved in a 1:1 mixture by volume of dimethylformamide-*d*<sub>7</sub> and water, pH 2.5) at three temperatures. The spectra were taken with the mixing time of 80 ms and with the spin-lock radio-frequency field, *B*<sub>1</sub>, of 3 kHz. The proton notation is given in Figure 3.

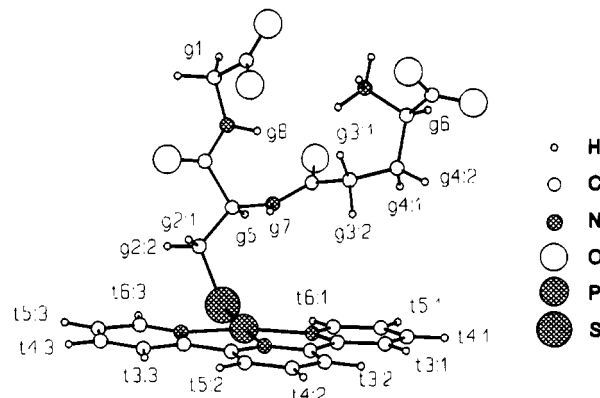


**Figure 3.** Structure of [Pt(trpy)GS]<sup>+</sup> at –15 °C in the cryoprotective solvent (1:1 mixture by volume of dimethylformamide-*d*<sub>7</sub> and water, pH 2.5), as determined by molecular energy minimization (CHARMM) of the XPLOR structures in which interligand distances were constrained by the results of NOE measurements.

in dimethylformamide, this complex salt was dissolved in a 1:1 mixture by volume of water and dimethylformamide. At –15 °C, the correlation time of molecular motion was long enough ( $\tau_c > 1$  ns) to allow observation of strong NOE between the terpyridine and glutathione protons in the ROESY spectrum (Figure 2). Multiple interligand NOE cross-peaks indicate that the two ligands are proximate in space. The most interesting cross-peaks are those between the  $\gamma$ -glutamyl methylene protons in the glutathionato ligand (1.9–2.5 ppm) and proton no. 5 in a terminal pyridine ring of the terpyridyl ligand (7.9 ppm). These cross-peaks persisted over the range of temperature (–20 to +20 °C), and their relative intensity reached a maximum at –2 °C. The structure (see Figure 3) was determined on the basis of the data collected at –15 °C, where the largest number of NOE contacts could be measured.

The ratio of NOESY and ROESY cross-relaxation rates was  $-1/2$  throughout the molecule, an indication that the spin-diffusion limit was reached. Distances between the geminal

(35) Piantini, U.; Sorensen, O. W.; Ernst, R. R. *J. Am. Chem. Soc.* **1982**, *104*, 6800–6801.

(36) Brooks, B. R.; Bruccoleri, R. E.; Olafson, B. D.; States, D. J.; Swaminathan, S.; Karplus, M. *J. Comput. Chem.* **1983**, *4*, 187–217.

(37) Jennette, K. W.; Gill, J. T.; Sadownik, J. A.; Lippard, S. J. *J. Am. Chem. Soc.* **1976**, *98*, 6159–6168.

(38) Ferraro, J. R. *Low-Frequency Vibrations of Inorganic and Coordination Compounds*; Plenum Press: New York, 1971.

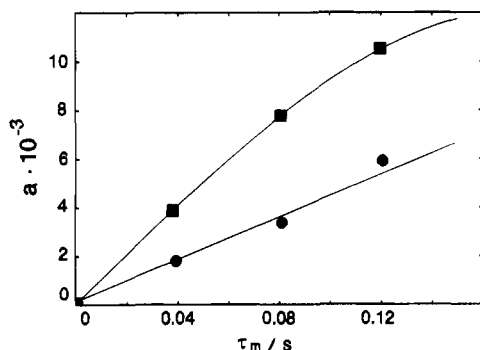
(39) Brunger, A. T. *X-PLOR*; Yale University Press: New Haven, CT, 1992.

(40) Raridon, R. J.; Kraus, K. A. Viscosities and Densities of Organic–Water Mixtures. In *Water Research Program 11.88*; Office of Saline Water Resources & Dev. Prog. Report 302; Office of Saline Water Resources & Dev. Prog. Report: 1968; pp 52–55.

**Table 1.** NOESY Cross-Relaxation Rates ( $\sigma^a$ ) of Proton Pairs at Fixed Distances ( $r$ ) and Also Correlation Times ( $\tau_c$ ) Calculated Assuming Isotropic Motion of the Rigid Molecule [Pt(trpy)GS]<sup>+</sup>

proton pair <sup>a</sup>	$\sigma^a$ (s <sup>-1</sup> )	$r$ (Å)	$10^{-2}\sigma^a r^6$ (s <sup>-1</sup> Å <sup>6</sup> )	$\tau_c$ (ns)
t6 and t5	1.5	2.45	3.2	5.6
t5 and t4	1.4	2.45	3.0	5.3
g2:1 and g2:2	10	1.75	2.9	5.1
g3:1 and g3:2	9.5	1.75	2.7	4.8
g4:1 and g4:2	9.8	1.75	2.8	5.0

<sup>a</sup> Notation is given in Figure 3.

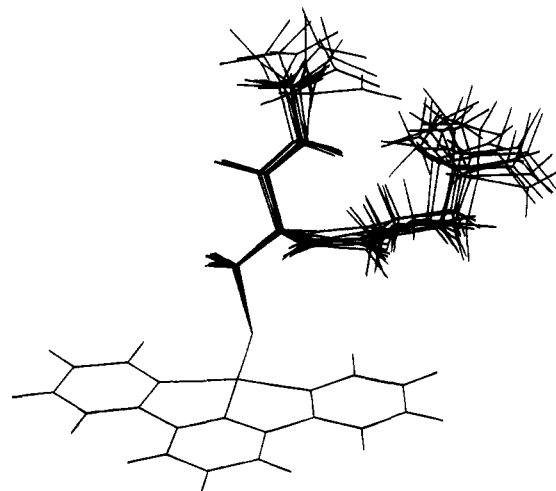
**Figure 4.** Dependence of normalized cross-peak intensities ( $a$ ) on the mixing time ( $\tau_m$ ). NOESY (●) and ROESY (■) buildup curves of the cross-peak between the glutamyl proton g3:2 and the terpyridine proton t5:1 in [Pt(trpy)GS]<sup>+</sup>, at -2 °C, at which the hydrophobic interaction is strongest. The proton notation is given in Figure 3.

protons in the glutathionato ligand and distances among the protons in the terpyridyl ligand are constant. If adjacent protons undergo the same motion, then product of their cross-relaxation rate and interproton distance is constant:  $\sigma_{klr} = f(\tau_c)$  according to eq 1. As Table 1 shows, this is the case. Since the five proton pairs under consideration are distributed over the entire [Pt(trpy)GS]<sup>+</sup> molecule and since they have various orientations, the molecule seems to move isotropically and as a rigid body. With these assumptions, an isotropic correlation time of about 5 ns is calculated (Table 1). The values of vicinal coupling constants in Table 2 also support the notion of isotropic motion of a rigid molecule, except at the ends of the glutathionato ligand. There, vicinal couplings between g1 and g5 and between g6 and g4 have a motionally averaged values of 5.5 and 6.7 Hz, respectively.

A series of NOESY and ROESY spectra was recorded with mixing times of 0, 20, 40, 80, and 120 ms. Volumes of cross-peaks were normalized by volumes of the corresponding diagonal peaks. Buildup curves of normalized cross-peak volumes were fitted to a quadratic function of the mixing time according to eq 4. A typical curve is shown in Figure 4.

Thirty-two nontrivial interproton distance that may be affected by conformational changes were determined from cross-relaxation rates, which were calculated with eq 6 using geminal methylene protons as the standard ( $\sigma_{std} = -10$  s<sup>-1</sup> and  $r_{std} = 1.75$  Å in Table 1). Fourteen of the distances (Table 2) are interligand ones. A few torsional angles in Table 2 were determined from vicinal couplings measured in 1D spectrum.

For the restrained molecular dynamic calculation, seven conformations of the complex [Pt(trpy)GS]<sup>+</sup> were prepared by the minimization of the randomized atomic coordinates. Each random conformation was used as an initial conformation for the simulated annealing that yielded 30 structures. The final ensemble of 210 conformations obtained by the annealing was analyzed with respect to deviation from the NOE distance restraints. Ten XPLOR structures with the lowest root-mean-square deviations (rms ~ 0.27) are shown in Figure 5. These structures also satisfy measured coupling constants. As it is

**Figure 5.** Ten structures of [Pt(trpy)GS]<sup>+</sup> with the lowest RMS deviations from experimental NOE distances (taken at -15 °C in the cryoprotective solvent), as determined by restrained molecular dynamics in XPLOR.

seen, the conformation of glutathionato ligand is well defined by the NOE restraints. The distribution of rotamers at glutathionato ends is in accordance with the averaged values of the vicinal couplings between g1 and g5 and between g6 and g4 protons. Molecular energy minimization of the structures in CHARMm resulted in a single conformation (Figure 3).

The chemically equivalent protons of the terpyridyl ligand are degenerate, therefore two almost opposite orientations of the glutathionato ligand with respect to the terpyridyl ligand were possible. However, the orientation exhibited in Figure 5 satisfied all NOE much better than the other one.

**Description of the [Pt(trpy)GS]<sup>+</sup> Structure and of the Glutathione Conformation.** The complex, in the cryoprotective solvent at -15 °C, has a compact conformation in which the glutamyl residue in the glutathionato ligand lies over a terminal pyridine ring in the terpyridyl ligand. The closest distance between the glutamyl aliphatic chain and the aromatic ligand (g3:2 to t5:1) is about 3.5 Å. There is an electrostatic attraction between the glycyl carboxyl and glutamyl amino groups, which favors the single conformation presented in Figure 3. However, as the vicinal couplings show, terminal groups of the glutathionato ligand rotate around the glycyl N-C<sub>α</sub> and glutamyl C<sub>β</sub>-C<sub>γ</sub> bonds, so the set of structures presented in Figure 5 describes the molecular conformation more realistically.

The shape of free glutathione in the crystal resembles an extended letter Y, with the cysteine side chain as the "stem of the fork".<sup>41</sup> Both NMR spectroscopic experiments and theoretical calculations indicate that a similar conformation predominates in solution as well.<sup>42</sup> In the most stable conformation of the zwitterion the glutamyl α-amino and γ-carbonyl groups electrostatically attract each other.<sup>42,43</sup>

According to a detailed NMR spectroscopic study,<sup>17</sup> the free zwitterion in aqueous solution at 30 °C exists in a large number of rotamers. The "most probable conformer", calculated from the NMR spectroscopic results, accounts for only 2.3% of all rotamers.

Conformation of the glutathionato ligand in [Pt(trpy)GS]<sup>+</sup> dissolved in a viscous solvent at -15 °C is Y-shaped, but it is more compressed (less extended) than the conformations of the free glutathione discussed above. The coordinated tripeptide differs greatly from the most stable or the most probable

(41) Wright, W. *Acta Crystallogr.* **1958**, *11*, 632-642.

(42) York, M. J.; Beilharz, G. R.; Kuchel, P. W. *Int. J. Pept. Protein Res.* **1987**, *29*, 638-646.

(43) Laurence, P. R.; Thomson, C. *Theor. Chim. Acta* **1980**, *57*, 25-41.

**Table 2.** Proton–Proton Distances (Å) Determined from NOE Cross-Relaxation Rates and Torsional Angles (deg) Determined from Vicinal Couplings<sup>a</sup>

interligand <sup>b</sup>	distance	intraligand	distance	torsion	angle	<sup>3</sup> J (Hz)
t6:1–g3:1	4.8	g1–g5	4.5	g2:1–C–C–g5	50 ± 10	5
t6:1–g3:2	4.0	g1–g8	2.6	g2:2–C–C–g5	170 ± 10	12
t6:1–g4:1	>5	g2:1–g5	2.4	g5–C–N–g7	150 ± 10	7.7
t6:1–g4:2	4.5	g2:2–g5	2.7	g3:2–C–C–g4:1	10 ± 10	10
t6:1–g5	3.0	g2:2–g7	2.7	g3:1–C–C–g4:2	230 ± 10	10
t6:1–g6	>5	g3:1–g6	3.2			
t6:1–g7	3.5	g3:1–g7	2.5			
t5:1–g3:1	4.5	g3:1–g4:1	2.7			
t5:1–g3:2	3.5	g3:1–g4:2	2.9			
t5:1–g4:1	3.8	g3:2–g4:1	2.6			
g5:1–g4:2	4.2	g3:2–g4:2	2.7			
t5:1–g5	>5	g3:2–g6	3.8			
t6:3–g2:1	2.6	g3:2–g7	2.4			
t6:3–g2:2	2.6	g4:1–g6	2.9			
		g4:2–g6	2.8			
		g5–g7	2.8			
		g5–g8	2.5			
		g7–g6	4.5			
		g7–g4:2	4.4			
		g7–g8	3.1			

<sup>a</sup> Notation is given in Figure 3. <sup>b</sup> The terpyridine protons are assigned according to molecular simulation restrained by the NOE results.

conformation of the free tripeptide in aqueous solution at or near room temperature. Except for the aforementioned GS–trpy hydrophobic interaction, in this square-planar complex ion there are no steric constraints that would prevent the tripeptide from adopting the extended Y-shape. We conclude that it is this hydrophobic interaction that stabilizes the compressed Y-shaped conformation.

On the basis of the available results, we cannot decide to what extent the difference in conformation between free glutathione and the glutathionato ligand in [Pt(trpy)GS]<sup>+</sup> is caused by coordination to the metal atom and by a change from an aqueous solution at room temperature to a viscous solution at –15 °C. Binding of gadolinium(III) to the carboxylate groups does not significantly change the conformational equilibrium of glutathione,<sup>17</sup> but this finding is not directly relevant to our study. Binding of Hg(II) and other metal ions to the cysteinato side chain has been studied by NMR spectroscopy,<sup>44</sup> but these studies did not deal with glutathione conformations. Possible conformational changes of glutathione upon metal binding to its cysteinato side chain can be examined only after more studies like the present one become available. We do, however, have clear evidence that the conformation of the coordinated glutathione is strongly affected by its interactions with coordinated terpyridine, the other ligand in [Pt(trpy)GS]<sup>+</sup>.

**Hydrophobic Ligand–Ligand Interaction.** The structure in Figure 5 may be governed by exclusion from the solvent of the most hydrophobic part of the glutathionato ligand, the glutamyl methylene groups, which are brought close to the aromatic terpyridyl ligand. In this position the glutamyl methylene groups are not available to the polar solvent (water), as inspection of NOE cross-peaks between the complex molecule and water (Figure 6) shows. There are strong cross-peaks between the water resonance on the one hand and g1, g5, and g6 aliphatic proton resonances in the glutathionato ligand on the other; but there are no cross-peaks between water and glutamyl protons g2, g3, and g4. There are cross-peaks between water and terpyridyl protons. Therefore, only those glutathionato protons that are facing the terpyridyl ligand (Figure 3) sit in a hydrophobic environment. This identification of hydrophobic interactions is possible for two reasons. First, disruption

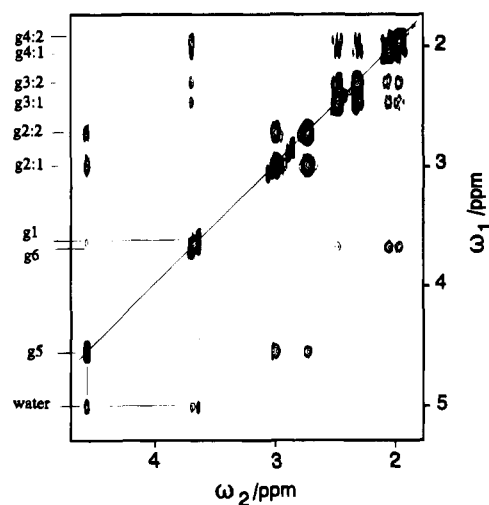


**Figure 6.** Aliphatic (glutathionato) proton resonances in a NOESY spectrum of [Pt(trpy)GS]<sup>+</sup> with a mixing time of 80 ms at –15 °C in the cryoprotective solvent. The central water signal was suppressed at low power (RF field of ~20 Hz) for 2.5 s. The proton notation is given in Figure 3.

of hydrogen bonding in water upon addition of dimethylformamide slows down the proton exchange among water molecules. Second, high viscosity and low temperature slow down the motion of solvent molecules.

Further evidence that conformation of the glutathionato ligand is governed by a hydrophobic interaction comes from the effect of temperature on the distance between the ligands involved in this interaction; see Figure 7. The closest approach of the glutamyl aliphatic chain (the proton g3:2) to the terpyridyl ligand (the proton t5:1) is ca. 3.3 Å at –2 °C; see Figure 3. The decrease in the interligand distance as the temperature increases from –20 to –2 °C reveals an interaction dominated by entropic factors. This is a hallmark of hydrophobic interactions. The structure is maintained by a tendency of more-ordered water surrounding the hydrophobic chain to become less-ordered bulk water as the temperature increases.<sup>45</sup>

**Implications for Enzymology of Glutathione.** A study of glyoxalase I led to a conclusion that glutathione derivatives

(44) Cheesman, B. V.; Arnold, A.; Rabenstein, D. J. *Am. Chem. Soc.* **1988**, *110*, 6359–6364.

(45) Urry, D. W. In *Proteins*; Renugopalakrishnan, V., Carey, P. R., Smith, I. C. P., Huang, S. G., Storer, A. C., Eds.; ESCOM Science Publishers B.V.: Leiden, The Netherlands, 1991; pp 352–360.

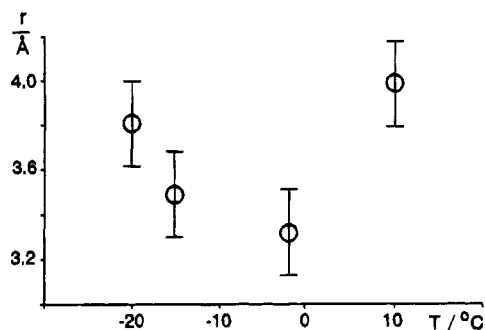
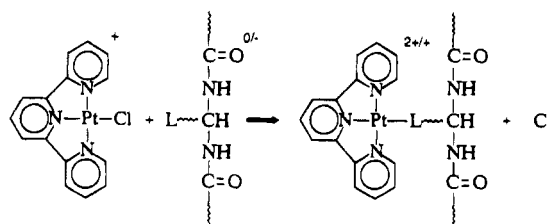


**Figure 7.** Temperature dependence of the distance,  $r$ , between the glutamyl methylene proton g3:2 and the terpyridyl proton t5:1 in  $[\text{Pt}(\text{trpy})\text{GS}]^+$ . The proton notation and the solvent are given in Figure 3 and its caption.

adopt an extended Y-shaped conformation when they are bound to this metalloenzyme and that the binding site is designed to accommodate a stable conformation of free glutathione.<sup>18</sup> Our study, however, shows that glutathione is susceptible to conformational change under the influence of hydrophobic interactions. Since these interactions often dominate association of enzymes with cofactors and substrates, the question of glutathione conformation when bound to glyoxalase I may be worth reconsidering.

**Interligand Interactions in Coordination Complexes and in Biomolecules.** In the laboratory of one of us the complex  $[\text{Pt}(\text{trpy})\text{Cl}]^+$  has been developed into a versatile and selective reagent for labeling of proteins and for reversible inhibition of certain enzymes.<sup>8-16,46,47</sup> Displacement of the chloride ligand by a nitrogen atom (in the neutral imidazole or guanidine group) or by a sulfur atom (in anionic thiolate group) results in stable and inert complexes of the  $\text{Pt}(\text{trpy})^{2+}$  tag with the coordinating side chains L, as shown schematically in Scheme 1. The  $[\text{Pt}(\text{trpy})\text{L}]^{2+/+}$  chromophores are easily detected and quantitated owing to the strong UV-vis absorption bands, which are due to electronic transitions within the aromatic terpyridine ligand and to platinum-to-terpyridine charge-transfer transitions.<sup>48</sup> The positions and relative intensities of these absorption bands depend not only on the identity of the protein-bound fourth ligand L (i.e., the side chain of histidine, cysteine, or arginine),

**Scheme 1**



but also on the environment in which the labeled amino acid residue sits. For example, the absorption patterns of the  $[\text{Pt}(\text{trpy})\text{His}]^{2+}$  chromophore are somewhat different when the labeled histidine residue is located in the hydrophobic or hydrophilic areas of the protein. Since charge-transfer absorption spectra are sensitive to polarity of the chromophore environment, these differences are quite useful. This stereochemical study indicates that the spectroscopic differences may arise from hydrophobic (and possibly other noncovalent) interactions between the  $\text{Pt}(\text{trpy})^{2+}$  group and the peptide that supplies the fourth ligand to the platinum(II) atom.

### Future Prospects

This study shows that the NOESY and ROESY NMR spectroscopic methods can be successfully applied to study of ligand-ligand interactions in coordination complexes. Cryoprotective mixtures as solvents hold promise in structural studies, by multidimensional NMR spectroscopy, of complexes that are models for metalloprotein active sites. Mixtures of water with alcohols, with dimethyl sulfoxide, and with dimethylformamide at low temperature have many properties in common with pure water at room temperature.<sup>49</sup> Partial ordering of these viscous solvents at low temperature resembles the state of water at interfaces with biological macromolecules.<sup>50</sup> This is the state of solvent at which the solvated biomolecule begins to assume preferred conformations.

**Acknowledgment.** We thank Professor Zhu Longgen for the synthesis of  $[\text{Pt}(\text{trpy})\text{GS}]\text{Cl}$ . The Analytical NMR Facility at Mayo Foundation is supported by the Grainger Foundation. The work at Iowa State University was supported by the National Science Foundation through the Grant CHE-9404971.

IC940818J

(46) Kostić, N. M. *Methods Enzymol.* **1993**, 226, 565-576.

(47) Ratilla, E. M. A.; Scott, B. K.; Moxness, M. S.; Kostić, N. M. *Inorg. Chem.* **1990**, 29, 918-926.

(48) Aldridge, T. K.; Stacy, E.; McMillin, D. *Inorg. Chem.* **1994**, 33, 722-727.

(49) Douzou, P.; Petsko, G. In *Advances in Protein Chemistry*; Anson, M., Edsall, J., Eds.; Academic Press: New York, 1984; pp 245-361.

(50) Motta, A.; Picone, D.; Tancredi, T.; Temussi, P. A. *J. Magn. Reson.* **1987**, 75, 364-370.